27th ABCM International Congress of Mechanical Engineering
December 04-08, 2023, Florianópolis-SC, Brazil

COB-2023-0152
FATIGUE LIFE PREDICTION OF MEDIUM CARBON STEEL WITH AN ARTIFICIAL DEFECT BASED ON SMALL CRACK GROWTH RELATION

Nathalia Manes Santos
Fábio Comes de Castro
Department of Mechanical Engineering, University of Brasilia, 70910-900 Brasilia, DF, Brazil
nathalia.santos@unb.aluno.br; fabio.castro@unb.br

Abstract. *The influence of defects on the durability of components is important in fatigue design since their presence may reduce fatigue life. Studies have indicated that total fatigue life of a metal with a small defect is mainly occupied by the life required for a crack to propagate up to macroscopic size. Therefore, relations capable to describe small crack growth are useful for estimating the fatigue life. In this work, an experimental evaluation of the Nisitani relation for small fatigue crack growth is performed. Uniaxial fatigue tests were conducted on SAE 1045 steel with an artificial cylindrical hole with diameter and depth of 400 µm. The specimens were subjected to fully reversed tension-compression with stress amplitudes ranging from 250 to 160 MPa, resulting in number of cycles to failure from 10^4 cycles up to the run-out condition (10^7 cycles). Fatigue crack growth was accompanied by periodically interrupting the tests and measuring the crack length with a confocal laser microscope. It was found that half of the fatigue life was spent on small crack growth until the crack reaches 1.5 mm. Also, the results indicated Nisitani relation could provide satisfactory live estimates up to 5×10^5 cycles, but it was not accurate on predicting fatigue lives longer than 10^6 cycles.*

Keywords: *fatigue life, small fatigue crack growth, microdefects, SAE 1045 steel.*

1. INTRODUCTION

Fatigue damage can be viewed as a progressive crack growth process. In this context, the total fatigue life can be divided into two periods. The first one is called crack initiation and is the number of cycles required for the appearance of a visible (macroscopic) crack. The period of long crack encompasses the life during which the a macrocrack propagates up to a critical size, ultimately leading to total fracture (Miller, 1993). Moreover, crack initiation can be further broken down into crack nucleation, microstructurally crack growth, in which the crack length is comparable to a grain size, and small crack growth, growth characterized by crack lengths from 0.5 to 2 mm (McDowell & Bennett, 1996).

Some researchers (Davidson et al., 2003; Kitagawa & Takahashi, 1976; McDowell & Bennett, 1996; Nisitani & Goto, 1986; Schijve, 1967) have highlighted that most of fatigue life is spent on small crack growth. Additionally, this phase becomes more predominant in materials that containing defects (Nourian-Avval & Fatemi, 2021). Since defects act as stresses concentrators, the crack nucleation occurs very quickly, so this phase can be neglected. Also, the period of long crack may be less significant compared with total fatigue life. As a result, small crack growth predictions may offer approaches for estimating the fatigue life.

Considering the aforementioned phenomenology, researchers have proposed models to predict small crack growth. However, unlike large crack growth, small crack growth is not determined by the stress intensity factor (ΔK), i.e. linear elastic fracture mechanics concepts are inappropriate to describe the growth of small cracks (Kitagawa & Takahashi, 1976; Pearson, 1975). This limitation occurs because the small scale yielding condition is not satisfied, in general, in the initial stages of crack development (Kawagoishi et al., 2000; Nisitani & Goto, 1986). Morevoer, small cracks are highly influenced by microstructure barriers such as grain boundaries (McDowell & Bennett, 1996; Miller, 1993; Schijve, 2009), making its growth irregular. This complex behavior poses difficulties in the development of a model capable of accurately describing small crack advance.

One of the attempts to model small crack growth was made by Nisitani (Goto & Nisitani, 1994; Kawagoishi et al., 1992, 2000; Nisitani et al., 1992; Nisitani & Goto, 1986). He proposed a unifying crack growth model, which covered both small and large cracks. He affirmed that large crack growth is determined by stress intensity factor range (ΔK), whereas small crack growth is uniquely determined by the parameter $\sigma_a^m l^n$, where σ_a is the stress amplitude, l is the crack length and m and n are material constants. Also, the author observed that the first relation is valid when the stress amplitude is relatively low compared to the yield stress (σ_y), approximately bellow of 0.5 σ_y, and, for higher stresses, the second relation holds. The equation form for Nisitani's model is as follows:

$$\frac{\mathrm{d}l}{\mathrm{d}N} = D(\Delta \mathrm{K})^q \text{ for large cracks } (\sigma_\mathrm{a} \leq 0.5\sigma_\mathrm{y}) \tag{1}$$

$$\frac{\mathrm{d}l}{\mathrm{d}N} = C\sigma_\mathrm{a}^m l^n \text{ for small cracks } (\sigma_\mathrm{a} \geq 0.6\sigma_\mathrm{y}) \tag{2}$$

In the present study, Nisitani's approach is used to predict the fatigue life of SAE 1045 steel specimens containing an artificial small hole. The fatigue tests were conducted under fully reversed tension-compression and covered lives from 10^4 cycles to run-out condition (10^7 cycles). Crack growth was observed by periodically interrupting the test and measuring the crack length. The experimental data were used to assess the accuracy and limitations of the Nisitani relation.

2. EXPERIMENTAL WORK

The material investigated in this study was the SAE 1045 steel, whose chemical composition in weight percentage was 0.46 C, 0.66 Mn, 0.19 Si, 0.012 S, 0.022 P, balanced by Fe. The material was acquired in the form of cylindrical bars with a diameter of 19.05 mm. To relieve the residual stresses due to the manufacturing process, the bars were annealed at 850 ºC for 45 minutes. The monotonic tensile properties of the material were: Young's modulus of 216 GPa, lower yield stress of 326 MPa, ultimate tensile strength of 661 MPa, 31% reduction of area. The Vickers hardness, averaged from five measurements and using a load of 10 N, was 189 kgf/mm².

Cylindrical solid specimens (Figure 1) were machined in accordance with the ASTM standard E466 (ASTM, 2021). The surface of the specimens was ground using sandpapers with grit numbers ranging from 220 to 2500. Then, surface roughness was measured using an Olympus OLS4100 confocal laser scanning microscope. It complied with the maximum surface roughness of 0.2 µm specified in the ASTM standard E466 (ASTM, 2021). After griding, a cylindrical hole with diameter and depth of 400 µm was produced in the middle of the gage section with an end mill and a Vega Model MVU920 Vertical Machining Center. A micrograph of the artificial hole before testing is shown in Figure 2.

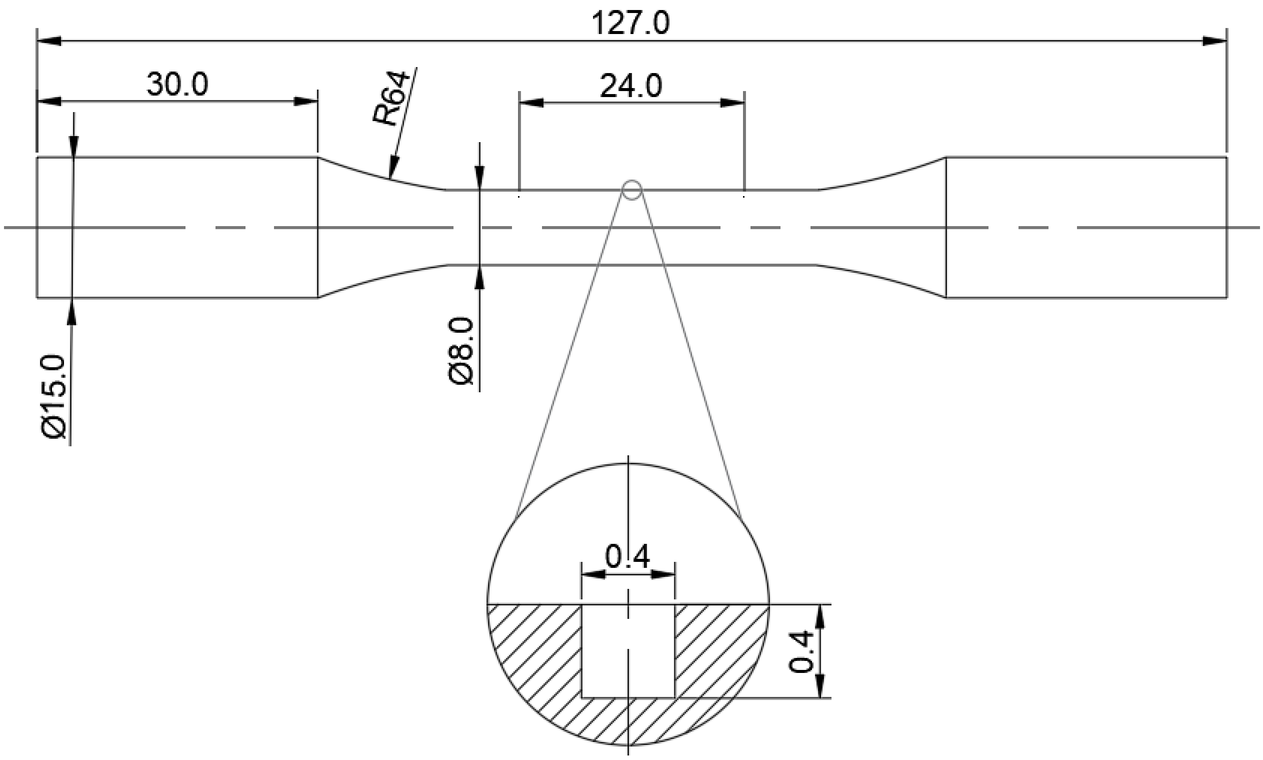

Figure 1. Specimen used in the fatigue tests (dimensions in mm)

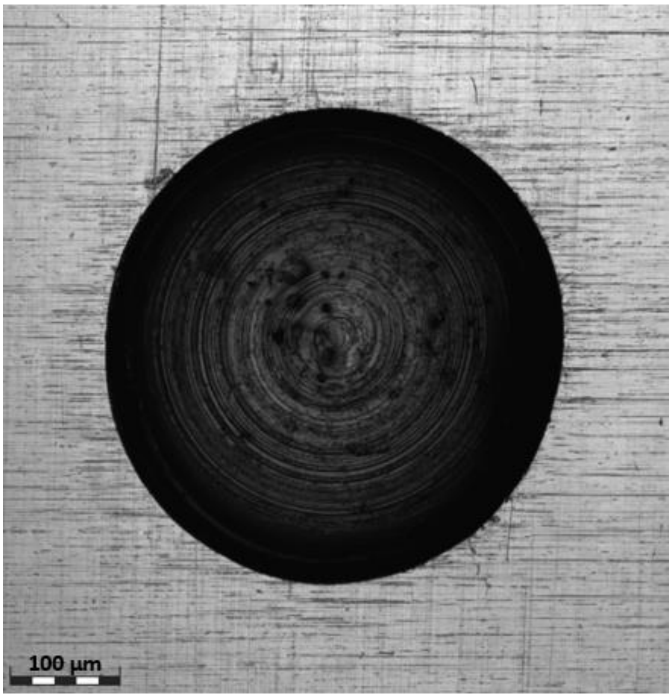

Figure 2. Micrograph of the artificial hole introduced into the specimen surface.

The fatigue tests were conducted under force control in an MTS servo-hydraulic machine with a capacity of 100 kN. The specimens were subjected to fully reversed tension-compression with stress amplitudes ranging from 160 MPa to 250 MPa. The tests were carried out until the total fracture of the specimen or were interrupted at the run-out condition (10^7 cycles). The S-N curve of the 1045 steel with microhole is presented in Figure 3.

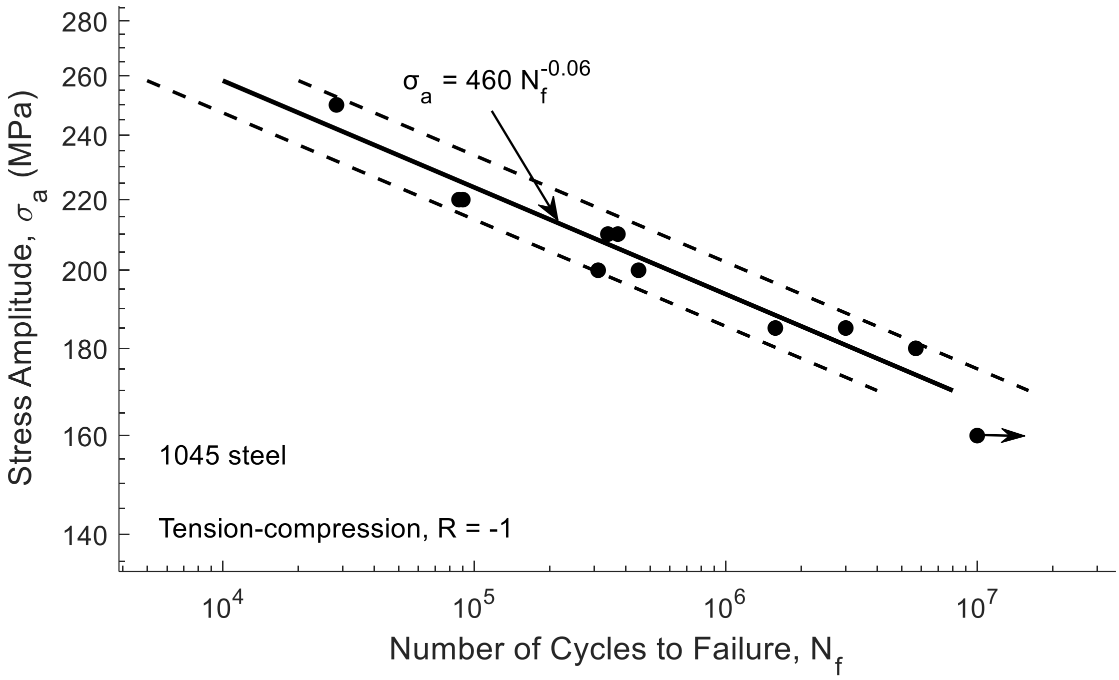

Figure 3. S-N data of 1045 steel with an artificial cylindrical hole (diameter and depth of 400 µm).

The evolution of crack length with number of cycles was determined by periodically interrupting the tests and measuring the crack length with the confocal laser scanning microscope. This equipment enabled the identification of an increase in crack length of, approximately, 10 µm. The cracks formed at the left and right sides of the hole were examined separately to enhance visibility and allow more accurate measurements. The total crack length was calculated by summing the hole diameter, the left crack length, and the right crack length. Figure 4 shows representative micrographs of the fatigue cracks emanated from the hole. The pictures were captured during the experiment conducted at the stress amplitude of 250 MPa after 9500 cycles. For this case, the total crack length is 632 µm. The crack growth rate, dl/dN, was determined by implementing the incremental polynomial method. This method entails fitting a second-order polynomial to 5 successive data points (ASTM, 2023).

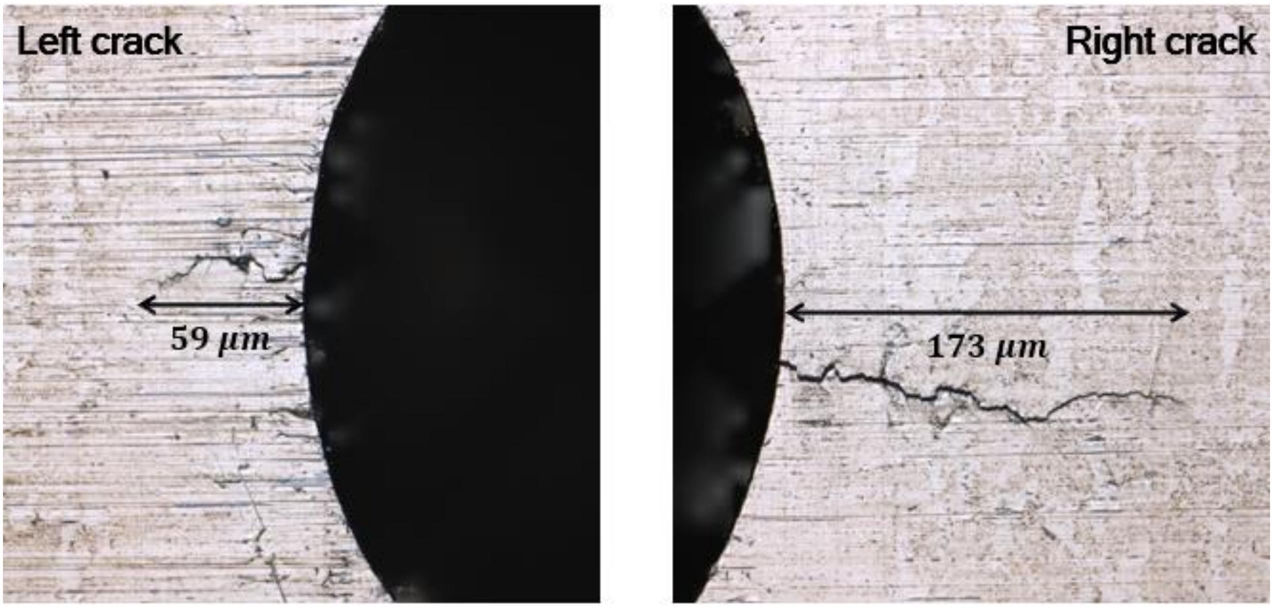

Figure 4. Fatigue cracks in the vicinity of the microhole observed in the experiment conducted at stress amplitude of 250 MPa, after 9500 loadings cycles.

3. RESULTS AND DISCUSSION

Figure 5(a) shows the relation between the crack length and the fatigue life fraction. A visible crack was first detected at $N/N_f = 0.2$. Additionally, it was observed that 70% of the fatigue life is required for a crack propagate up to 1.5 mm. Therefore, a significant portion of the fatigue life (approximately 50%) is spent on small crack growth phase. Figure 5 (b) shows the crack growth rate (dl/dN) versus the crack length. The slope of the line is the constant n in Nisitani model, which is approximately 1 for all stress amplitudes. This relation described well the experimental data at higher stress amplitudes, where the crack growth rate followed a linear trend in the log-log diagram without significant fluctuations. However, in tests performed at lower stress amplitudes, crack growth rate exhibited irregular behavior. This irregularity can be attributed to the stronger influence of microstructural barriers, such as grain boundaries. It should be noted that Nisitani performed tests with SAE 1045 steel submitted to different heat treatments, considered defects with dimensions different than that in the present study and used the plastic replication technique for crack length measurement. Despite all these differences, Nisitani also obtained a slope $n = 1$ in his study (Nisitani & Goto, 1986).

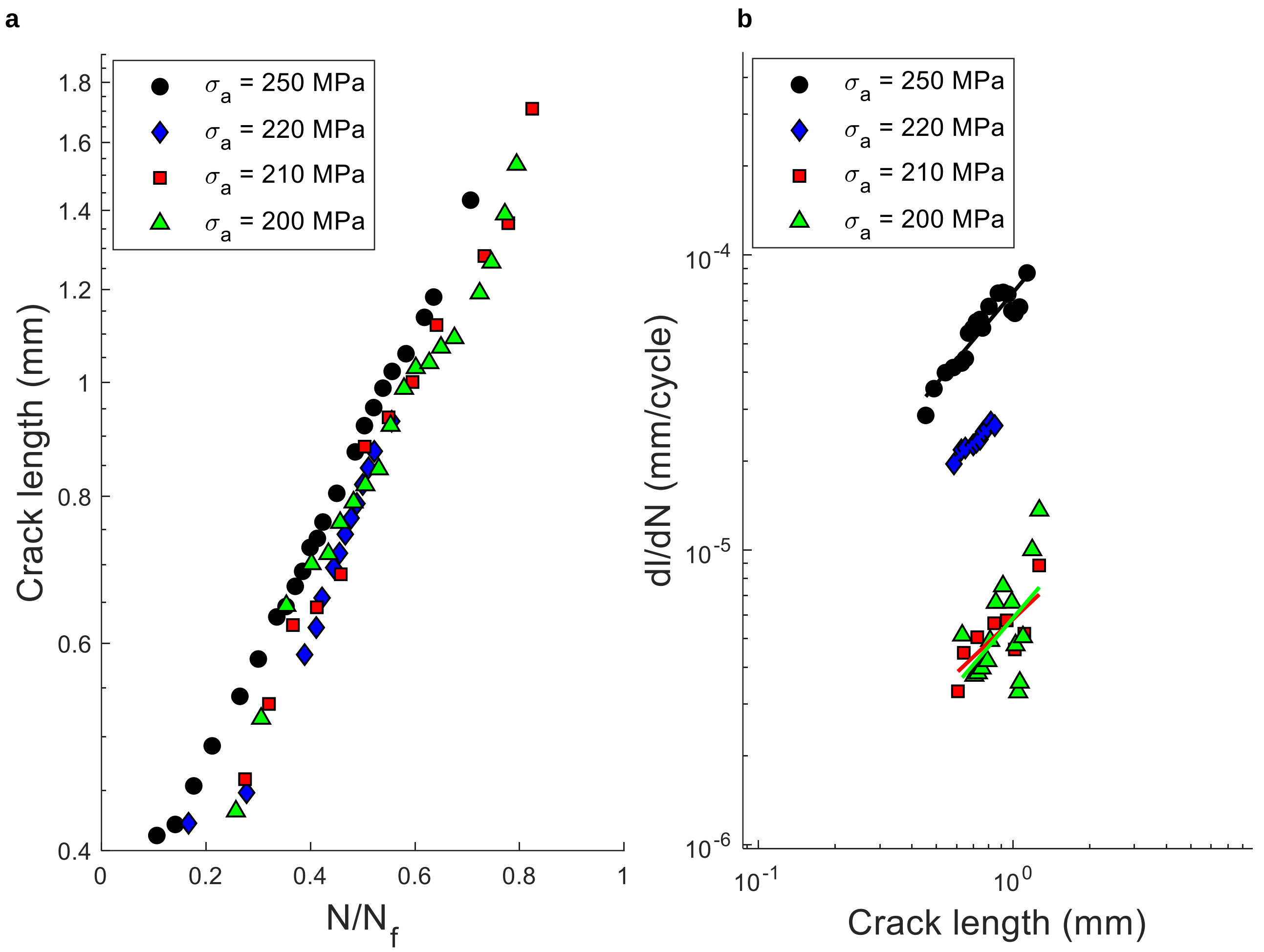

Figure 5. (a) Crack length versus fatigue life fraction and (b) Crack growth rate versus crack length.

The constants *m* and *C* in Nisitani relation can be found by best fitting a line to dl/dN versus $\sigma_a^m l^n$ data in logarithmic scales (Figure 6). This procedure yielded m = 6.3 and C = 4.83×10^{-20}. Due to the irregular crack growth behavior in experiments under lower stress amplitudes (σ_a = 200 MPa and σ_a = 208.5 MPa), such tests were considered unsuitable for model calibration. Therefore, only data from experiments conducted at highest stresses amplitudes (σ_a = 250 MPa and σ_a = 220 MPa) were used for this purpose.

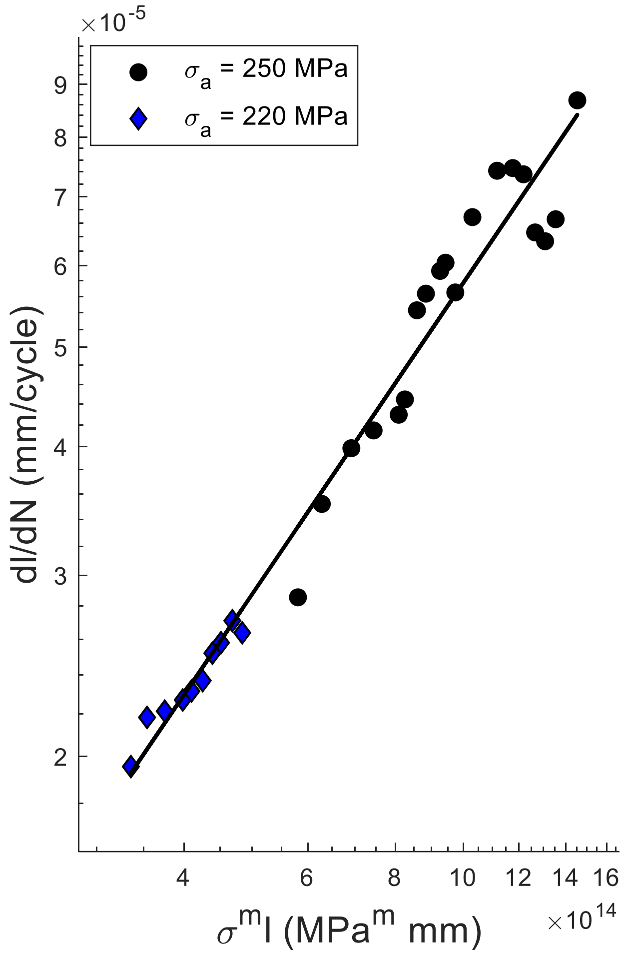

Figure 6. Crack growth rate versus $\sigma_{\mathrm{a}}^{m} l^{n}$ for the tests conducted at high stress amplitudes (σ_{a} = 220 MPa and σ_{a} = 250 MPa)

Fatigue life can be estimated by integrating the Nisitani relation from 0.4 mm (the diameter of the crack-like hole) to a macroscopic size of, say, 1.5 mm. Therefore,

$$N = \int_{l_i}^{l_f} C\sigma_{\mathrm{a}}^{m} l^{n} \mathrm{d}l = \frac{1}{C\sigma_{\mathrm{a}}^{m}}\left(ln\frac{l_f}{l_i}\right)^{n} \tag{3}$$

where $C = 4.83\times10^{-20}$, $m = 6.3$, $n = 1$, $l_i = 0.4$ and $l_f = 1.5$.

To validate the accuracy of the model, the authors applied it to the fatigue test data. As shown in Figure 7(a), the predictions are not in good agreement with the experimental results. The margin of error considered was 4, which could be acceptable if it covered all of points. The discrepancy is greater for longer life tests, for which the model tends to be more conservative. This can be attributed to the model calibration, which was based on test data produced at higher stress amplitudes. Therefore, it is reasonable to expect that the model performs more accurately in experiments with shorter life.

However, it was observed that approximately 50% of the fatigue life is spent in small crack growth. So, the authors proposed using the model for predicting half of the fatigue life. The results are shown in Figure 7(b), and they are in better agreement with experimental results. It can be observed by the reduce of the margin of error to 3. Even though, for longer life tests, the model is still inaccurate.

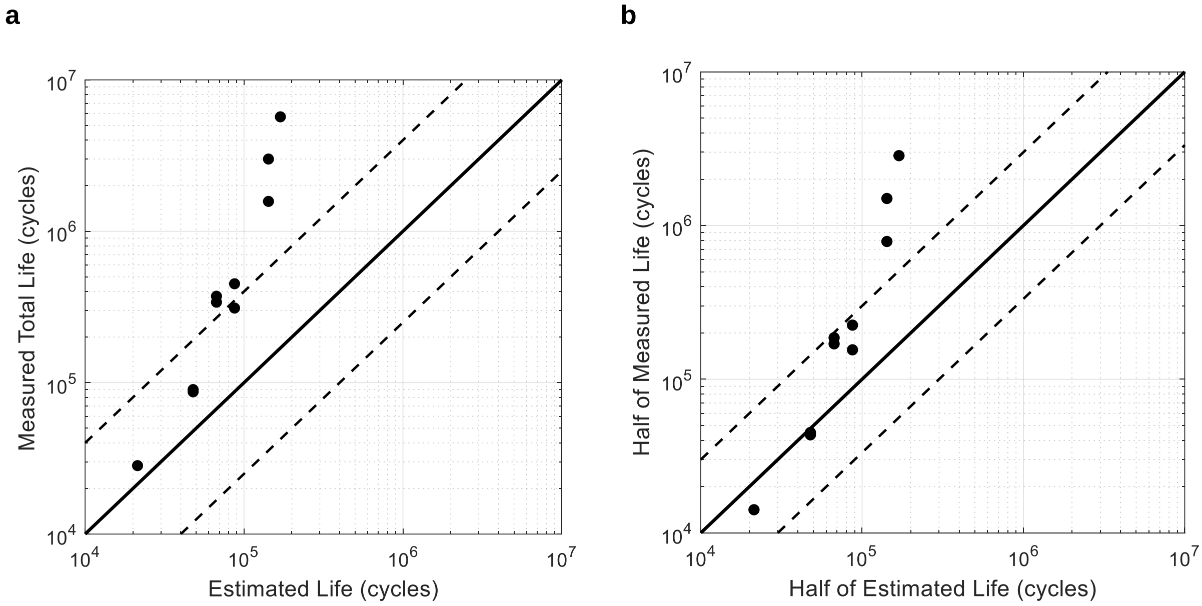

Figure 7. Fatigue lives estimated using the Nisitani relation compared with (a) measured total life and (b) half of the measured total life.

4. CONCLUSIONS

Measurement of the length of small cracks (from 10 µm up to 1.5 mm) using a confocal laser microscope provided a viable alternative to the plastic replication method, commonly used for monitoring small crack growth. The crack growth data of SAE 1045 steel with a small hole indicated that fatigue life was mostly spent in crack growth up to 1.5 mm. The data obtained from crack growth was used for predicting fatigue life. The prediction of the total fatigue life using the Nisitani relation resulted in reasonably accurate life estimates up to 5×10^5 cycles. For longer fatigue lives, predictions were not satisfactory.

5. REFERENCES

ASTM. (2021). *Standard Practice for Conducting Force Controlled Constant Amplitude Axial Fatigue Tests of Metallic Materials*. ASTM International. https://doi.org/10.1520/E0466-21.2

ASTM. (2023). *Standard Test Method for Measurement of Fatigue Crack Growth Rates*. ASTM International. https://doi.org/10.1520/E0647-23

Davidson, D., Chan, K., McClung, R., & Hudak, S. (2003). Small Fatigue Cracks. In *Comprehensive Structural Integrity* (Vol. 4, Issue April, pp. 129–164). https://doi.org/10.1016/B0-08-043749-4/04073-8

Goto, M., & Nisitani, H. (1994). Fatigue Life Prediction of Heat-Treated Carbon Steels and Low Alloy Steels Based on a Small Crack Growth Law. *Fatigue & Fracture of Engineering Materials & Structures*, *17*(2), 171–185. https://doi.org/10.1111/j.1460-2695.1994.tb00799.x

Kawagoishi, N., Chen, Q., & Nisitani, H. (2000). Significance of the small crack growth law and its practical application. *Metallurgical and Materials Transactions A: Physical Metallurgy and Materials Science*, *31*(8), 2005–2013. https://doi.org/10.1007/s11661-000-0228-6

Kawagoishi, N., Nisitani, H., & Toyohiro, T. (1992). Minimum Fatigue Crack Length for the Application of Small-Crack Growth Law. *JSME International Journal*, *35*(1), 234–240.

Kitagawa, H., & Takahashi, S. (1976). Applicability of fracture mechanics to very small cracks or the cracks in the early stage. *International Conference on Mechanical Behavior of Materials 2nd 760816*, *2*, 627–631.

McDowell, D. L., & Bennett, V. P. (1996). A microcrack growth law for multiaxial fatigue. *Fatigue & Fracture of Engineering Materials & Structures*, *19*(7), 821–837.

Miller, K. J. (1993). The two thresholds of fatigue behaviour. *Fatigue & Fracture of Engineering Materials & Structures*, *16*(9), 931–939. https://doi.org/https://doi.org/10.1111/j.1460-2695.1993.tb00129.x

Nisitani, H., & Goto, M. (1986). A Small-Crack Growth Law and its Application to the Evaluation of Fatigue Life. In *Life* (pp. 461–478).

Nisitani, H., Goto, M., & Kawagoishi, N. (1992). A small-crack growth law and its related phenomena. *Engineering Fracture Mechanics*, *41*(4), 499–513. https://doi.org/10.1016/0013-7944(92)90297-R

Nourian-Avval, A., & Fatemi, A. (2021). Fatigue performance and life prediction of cast aluminum under axial, torsion, and multiaxial loadings. *Theoretical and Applied Fracture Mechanics*, *111*(October 2020), 102842.

https://doi.org/10.1016/j.tafmec.2020.102842
Pearson, S. (1975). Initiation of fatigue cracks in commercial aluminium alloys and the subsequent propagation of very short cracks. *Engineering Fracture Mechanics*, *7*(2). https://doi.org/10.1016/0013-7944(75)90004-1
Schijve, J. (1967). Significance of Fatigue Cracks in Micro-Range and Macro-Range. *ASTM STP 415*, 415–459. https://doi.org/10.1520/stp47238s
Schijve, J. (2009). Fatigue Crack Growth. Analysis and Predictions. In *Fatigue of structures and materials* (pp. 209–256). Springer. https://doi.org/https://doi.org/10.1007/978-1-4020-6808-9_8